

H(125) bosonic decays in the ATLAS experiment

Higgs Hunting 2022

Ruggero Turra
on behalf of the ATLAS Collaboration

INFN Milano

12 September, 2022

1 Higgs boson and its properties

2 Decay channels ($\gamma\gamma$, $ZZ^* \rightarrow 4l$, $WW^* \rightarrow e\nu\mu\nu$)

3 The analyses

4 Results

Excess compatible with Higgs boson firmly established by ATLAS+CMS in 2012.

Measurements

- $\sigma \times BR$: for each production-mode, STXS region (very optimized analyses, acceptance extrapolation, larger SM assumption)
- Inclusive and differential fiducial cross sections (minimal model dependence)
- Mass: m_H known at $< 0.2\%$ (single channel), see talk by Siyuan Yan in the afternoon

Interpretations

- Spin and parity: 0^+ , other models excluded in Run 1
- CP structure (see talk by José Gonçalo tomorrow)
- Signal strengths: $\mu_i = \sigma_i/\sigma_i^{SM}$, $\mu_f = BR_f/BR_f^{SM}$ (inclusive, per-production-mode, ...)
- Coupling modifiers to SM particles (kappa-framework)
- EFT interpretations (see talk by Alexander Held tomorrow)

Excess compatible with Higgs boson firmly established by ATLAS+CMS in 2012.

Measurements

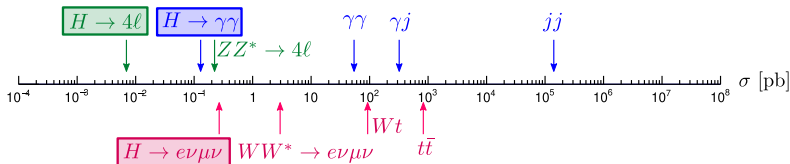
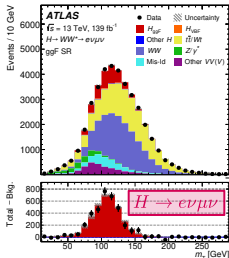
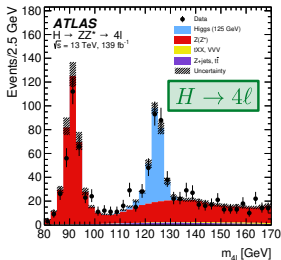
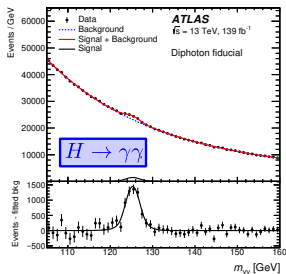
- $\sigma \times BR$: for each production-mode, STXS region (very optimized analyses, acceptance extrapolation, larger SM assumption)
- Inclusive and differential fiducial cross sections (minimal model dependence)
- Mass: m_H known at $< 0.2\%$ (single channel), see talk by Siyuan Yan in the afternoon

Interpretations

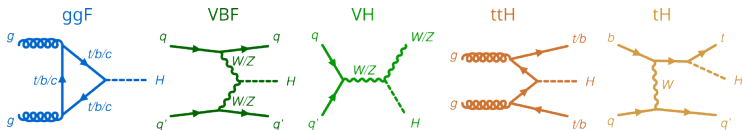
- Spin and parity: 0^+ , other models excluded in Run 1
- CP structure (see talk by José Gonçalo tomorrow)
- Signal strengths: $\mu_i = \sigma_i / \sigma_i^{SM}$, $\mu_f = BR_f / BR_f^{SM}$ (inclusive, per-production-mode, ...)
- Coupling modifiers to SM particles (kappa-framework)
- EFT interpretations (see talk by Alexander Held tomorrow)

$$\gamma\gamma, ZZ^* \rightarrow 4\ell, WW^* \rightarrow e\nu\mu\nu$$

	BR/ 10^{-3}	sig. eff.	mass resolution	Backgrounds
$\gamma\gamma$	2.27	39%	1.0–2.2 GeV	Large: $q\bar{q}/gg \rightarrow \gamma\gamma$
4ℓ	0.124	16-33%	1.6–2.4 GeV	Very small: $q\bar{q}/gg \rightarrow ZZ^*$
$e\nu\mu\nu$	5.04	$\sim 11\%$	Transverse mass	Medium: $q\bar{q}/gg \rightarrow WW^*, t\bar{t}, Wt$

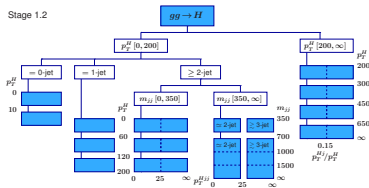


Higgs production and Simplified Template X-Sections (STXS)



- 1 Split cross sections by production modes
- 2 Split in exclusive regions of phase space, differently for each production modes

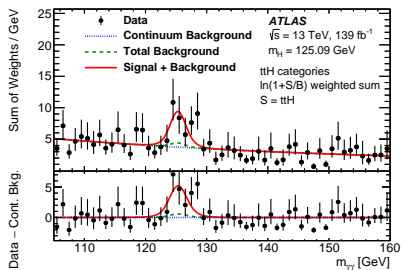
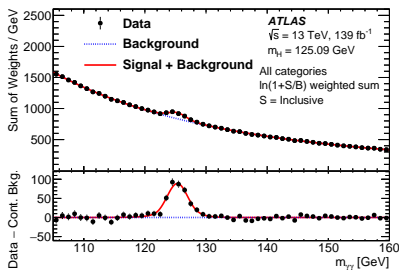
STXS maximize the sensitivity of the measurements while at the same time to minimize their theory dependence



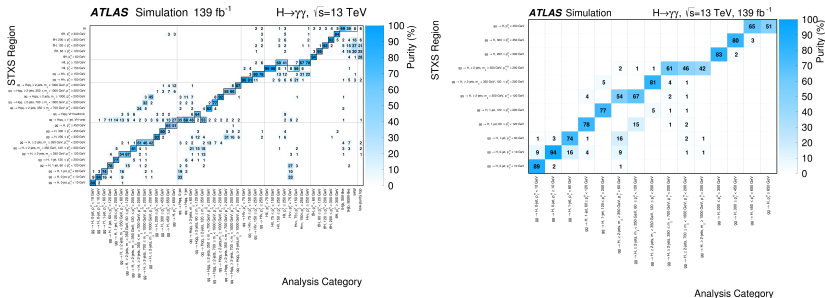
Going to show latest results by ATLAS with full Run2 (139 fb^{-1} at $\sqrt{s} = 13 \text{ TeV}$)

- 1 Select events to increase S/B
- 2 Split events into **categories** using reconstructed quantities, separating the sub-processes you want to measure (e.g. ggF vs VBF, different Higgs p_T ranges, ...)
- 3 Define **control regions** to constrain the yield of background processes
- 4 Quantify the efficiency and migrations for each sub-process and each category (e.g. $P[\text{ggF-category}|\text{true-VBF-process}]$, ...) with MC
- 5 Define an observable to estimate background from data (e.g. $m_{\gamma\gamma}$) and model it
- 6 Minimize a likelihood (matrix method unfolding) to simultaneously measure the cross-sections

- Using $m_{\gamma\gamma}$ as continuous observables
- **Signal shape** parametrized using a function fitted on simulations
- **Background shape** parametrized using a function fitted on data
 - The functional form is chosen with the **spurious signal** criteria: minimize the signal fitted on a background-only high-statistic simulation



- Measuring 28 STXS bins (45 considered in the design)
- Two steps:
 - A first multiclass BDT separating the signal sub-processes (the STXS bins)
 - Additional splitting to increase purity using a set of binary BDTs: **101 categories!**
- **Novel approach** based on **D-optimality**: minimize the determinant of the expected covariance matrix of the measurement
 - Implemented tuning a set of weights applied to the outputs of the multiclass
 - Simultaneous optimization for all the STXS bins

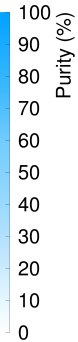
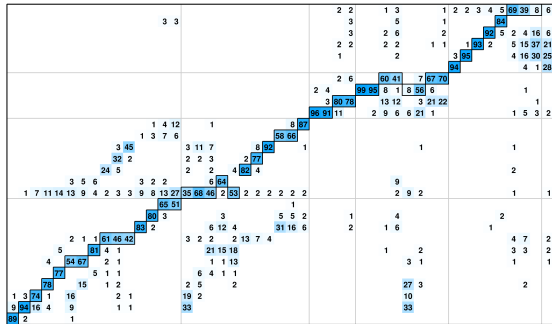


ATLAS Simulation 139 fb⁻¹

$H \rightarrow \gamma\gamma$, $\sqrt{s}=13$ TeV

STXS Region

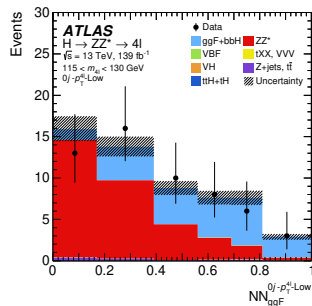
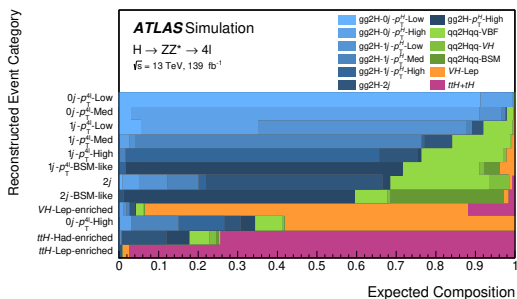
- ttH, $p_T^H \geq 300$ GeV
- ttH, $200 \leq p_T^H < 300$ GeV
- ttH, $120 \leq p_T^H < 200$ GeV
- ttH, $60 \leq p_T^H < 120$ GeV
- ttH, $p_T^H < 60$ GeV
- ttH, $p_T^H \geq 150$ GeV
- ttH, $p_T^H < 150$ GeV
- qq → ttH, $p_T^H \geq 150$ GeV
- qq → ttH, $p_T^H < 150$ GeV
- qq → ttH, ≥ 2 jets, $m_{\gamma\gamma} \geq 1000$ GeV, $p_T^H \geq 200$ GeV
- qq → ttH, ≥ 2 jets, $350 \leq m_{\gamma\gamma} < 1000$ GeV, $p_T^H \geq 200$ GeV
- qq → ttH, ≥ 2 jets, $m_{\gamma\gamma} \geq 1000$ GeV, $p_T^H < 200$ GeV
- qq → ttH, ≥ 2 jets, $700 \leq m_{\gamma\gamma} < 1000$ GeV, $p_T^H < 200$ GeV
- qq → ttH, ≥ 2 jets, $350 \leq m_{\gamma\gamma} < 700$ GeV, $p_T^H < 200$ GeV
- qq → ttH, VH hadronic
- qq → ttH, ≥ 1 jet, VH veto
- qq → ttH, $p_T^H \geq 450$ GeV
- gg → ttH, $300 \leq p_T^H < 450$ GeV
- gg → ttH, $200 \leq p_T^H < 300$ GeV
- gg → ttH, ≥ 2 jets, $m_{\gamma\gamma} \geq 350$ GeV, $p_T^H \geq 200$ GeV
- gg → ttH, ≥ 2 jets, $m_{\gamma\gamma} < 350$ GeV, $120 \leq p_T^H < 200$ GeV
- gg → ttH, ≥ 2 jets, $m_{\gamma\gamma} < 350$ GeV, $p_T^H < 120$ GeV
- gg → ttH, 1 jet, $120 \leq p_T^H < 200$ GeV
- gg → ttH, 1 jet, $60 \leq p_T^H < 120$ GeV
- gg → ttH, 1 jet, $p_T^H < 60$ GeV
- gg → ttH, 0 jet, $p_T^H \geq 10$ GeV
- gg → ttH, 0 jet, $p_T^H < 10$ GeV



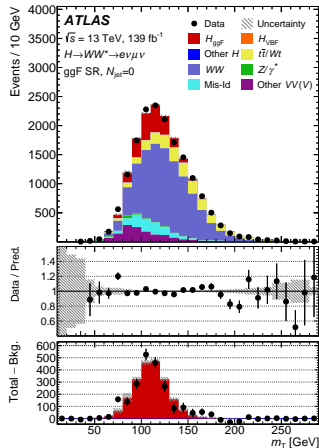
- gg → ttH, 0 jets, $p_T^H < 10$ GeV
- gg → ttH, 0 jets, $p_T^H \geq 10$ GeV
- gg → ttH, 1 jet, $p_T^H < 60$ GeV
- gg → ttH, 1 jet, $p_T^H \geq 60$ GeV
- gg → ttH, 1 jet, 605 $p_T^H < 120$ GeV
- gg → ttH, 1 jet, 1205 $p_T^H < 200$ GeV
- gg → ttH, 1 jet, 2005 $p_T^H < 300$ GeV
- gg → ttH, 1 jet, 3005 $p_T^H < 450$ GeV
- gg → ttH, ≥ 2 jets, $m_{\gamma\gamma} \geq 1000$ GeV, $p_T^H \geq 200$ GeV
- gg → ttH, ≥ 2 jets, $m_{\gamma\gamma} \geq 350$ GeV, $120 \leq p_T^H < 200$ GeV
- gg → ttH, ≥ 2 jets, $m_{\gamma\gamma} < 350$ GeV, $p_T^H \geq 200$ GeV
- gg → ttH, ≥ 2 jets, $350 \leq m_{\gamma\gamma} < 700$ GeV, $p_T^H \geq 200$ GeV
- gg → ttH, ≥ 2 jets, $700 \leq m_{\gamma\gamma} < 1000$ GeV, $p_T^H \geq 200$ GeV
- gg → ttH, ≥ 2 jets, $m_{\gamma\gamma} \geq 1000$ GeV, $p_T^H < 200$ GeV
- gg → ttH, $200 \leq p_T^H < 300$ GeV
- gg → ttH, $300 \leq p_T^H < 450$ GeV
- gg → ttH, $450 \leq p_T^H < 650$ GeV
- gg → ttH, $p_T^H \geq 650$ GeV
- gg → ttH, $p_T^H < 650$ GeV
- qq → ttH, 0 jet
- qq → ttH, 1 jet
- qq → ttH, ≥ 2 jets, $m_{\gamma\gamma} < 60$ GeV
- qq → ttH, ≥ 2 jets, $60 \leq m_{\gamma\gamma} < 120$ GeV
- qq → ttH, ≥ 2 jets, $120 \leq m_{\gamma\gamma} < 350$ GeV
- qq → ttH, ≥ 2 jets, $350 \leq m_{\gamma\gamma} < 700$ GeV, $p_T^H \geq 200$ GeV
- qq → ttH, ≥ 2 jets, $700 \leq m_{\gamma\gamma} < 1000$ GeV, $p_T^H \geq 200$ GeV
- qq → ttH, ≥ 2 jets, $m_{\gamma\gamma} < 1000$ GeV, $p_T^H \geq 200$ GeV
- qq → ttH, ≥ 2 jets, $m_{\gamma\gamma} < 200$ GeV
- qq → ttH, ≥ 2 jets, $350 \leq m_{\gamma\gamma} < 700$ GeV, $p_T^H < 200$ GeV
- qq → ttH, ≥ 2 jets, $700 \leq m_{\gamma\gamma} < 1000$ GeV, $p_T^H < 200$ GeV
- qq → ttH, ≥ 2 jets, $m_{\gamma\gamma} \geq 1000$ GeV, $p_T^H < 200$ GeV
- qq → ttH, $p_T^H < 75$ GeV
- qq → ttH, $75 \leq p_T^H < 150$ GeV
- qq → ttH, $150 \leq p_T^H < 250$ GeV
- qq → ttH, $p_T^H \geq 250$ GeV
- ttH, $p_T^H < 75$ GeV
- ttH, $75 \leq p_T^H < 150$ GeV
- ttH, $150 \leq p_T^H < 250$ GeV
- ttH, $p_T^H \geq 250$ GeV
- ttH, $p_T^H < 75$ GeV
- ttH, $75 \leq p_T^H < 150$ GeV
- ttH, $150 \leq p_T^H < 200$ GeV
- ttH, $200 \leq p_T^H < 300$ GeV
- ttH, $p_T^H \geq 300$ GeV
- ttH, $p_T^H < 60$ GeV
- ttH, $60 \leq p_T^H < 120$ GeV
- ttH, $120 \leq p_T^H < 200$ GeV
- ttH, $200 \leq p_T^H < 300$ GeV
- ttH, $p_T^H \geq 300$ GeV
- ttH, BSM-like
- ttH, BSM-like
- ttH
- low-purity top

Analysis Category

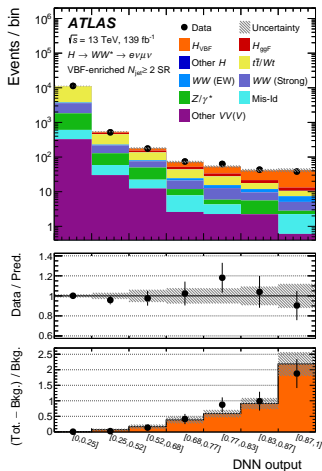
- Targeting 12 STXS 1.1 bins
- Main background from non-resonant ZZ , constrained from data sidebands
- Events split in 12 categories: first select ttH -like events, then split by jet multiplicity. Further splitting according to STXS.
- Fit to a new neural network discriminant. NN combine 2 RNN (for lepton and jet information) into a DNN.



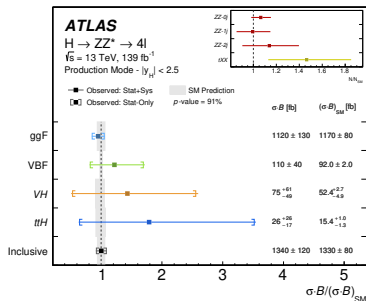
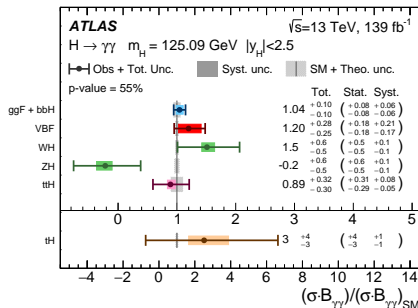
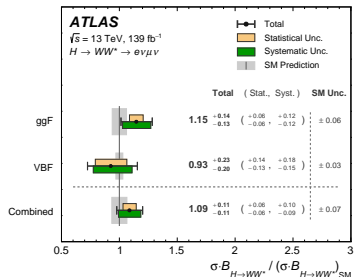
- Targeting **only ggF and VBF** and 11 STXS 1.2 bins
- Only different flavour. Categorization: 0jet, 1jet, ≥ 2 jets
 - Background composition different depending on jet multiplicity
 - Additional splitting to target STXS
- Background $qq \rightarrow WW$, top, $Z/\gamma^* \rightarrow \tau\tau$ predictions normalized using **several control regions**
- Simultaneous fit of signal and control regions, using m_T or DNN (ggF vs VBF) as observable

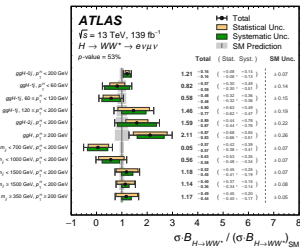
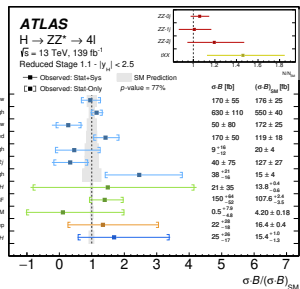
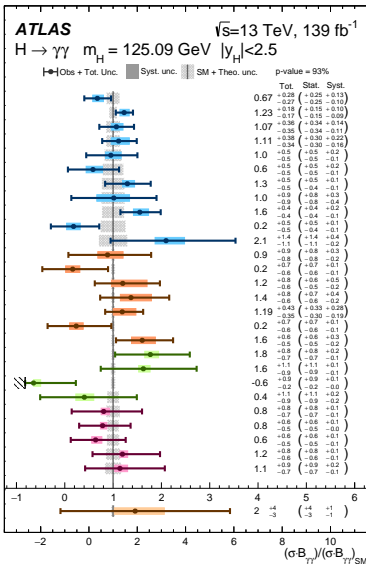


- Targeting **only ggF and VBF** and 11 STXS 1.2 bins
- Only different flavour. Categorization: 0jet, 1jet, ≥ 2 jets
 - Background composition different depending on jet multiplicity
 - Additional splitting to target STXS
- Background $qq \rightarrow WW$, top, $Z/\gamma^* \rightarrow \tau\tau$ predictions normalized using **several control regions**
- Simultaneous fit of signal and control regions, using m_T or **DNN** (ggF vs VBF) as observable

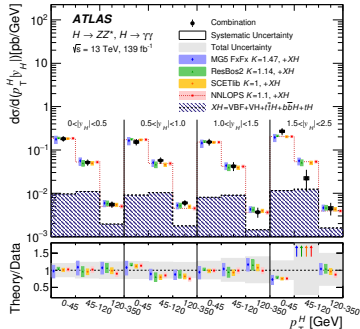
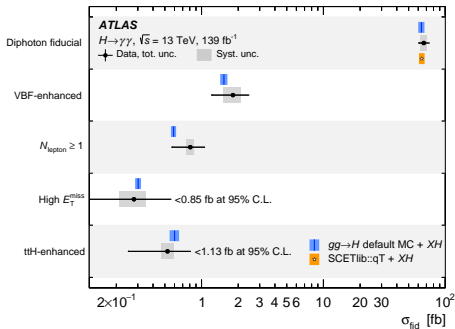


- Good agreement with SM
- $ggH \simeq 10\%$, $VBF \simeq 20\text{-}30\%$
- WW limited by systematics
- Non-negligible correlation between ggF/VBF , WH/ZH , tH/ttH

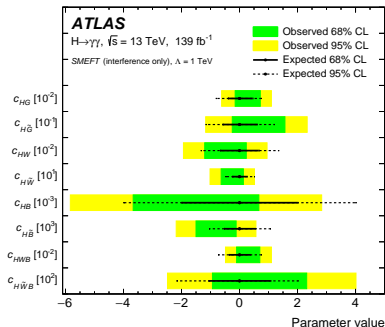




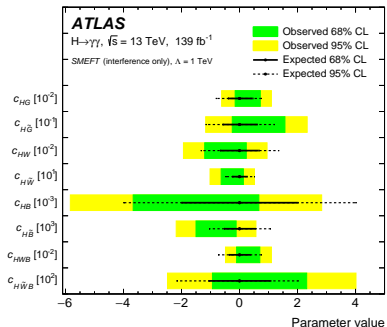
- Cross sections in fiducial space, defined by detector acceptance and trigger requirements
- Inclusive or (double) differential, also in smaller phase space to study non-ggF
- Unfolded with **matrix method** in the likelihood fit
- $\gamma\gamma/ZZ$ uses different phase space, so extrapolate to the full phase space in the combination (using SM assumptions)
 - $p_T, |y|, p_T$ vs $|y|, N_{jets}, p_{T,j1}$
 - many more cross-sections by single channels



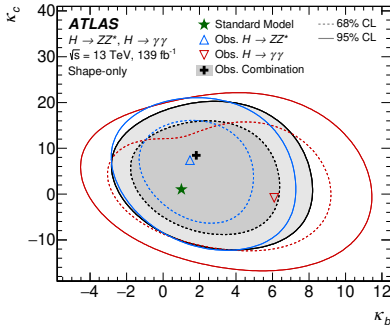
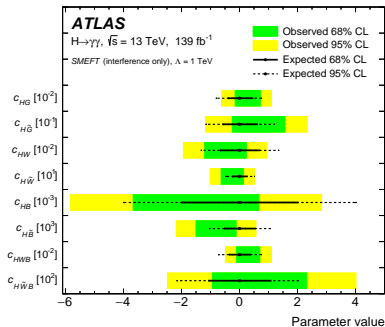
- $\gamma\gamma$: EFT constraints on Wilson coefficients
- ZZ : anomalous couplings to H and Z and contact interaction from left- and right-handed leptons to H using m_{12} and m_{34}
- Both: constraints on c - and b -quark Yukawa coupling using shape-only (or with normalization)



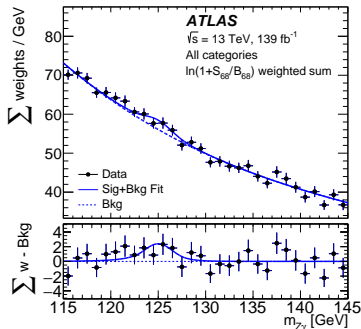
- $\gamma\gamma$: EFT constraints on Wilson coefficients
- ZZ: anomalous couplings to H and Z and contact interaction from left- and right-handed leptons to H using m_{12} and m_{34}
- Both: constraints on c - and b -quark Yukawa coupling using shape-only (or with normalization)



- $\gamma\gamma$: EFT constraints on Wilson coefficients
- ZZ : anomalous couplings to H and Z and contact interaction from left- and right-handed leptons to H using m_{12} and m_{34}
- Both: constraints on c - and b -quark Yukawa coupling using shape-only (or with normalization)



- Published Run2 results for STXS and fiducial cross sections are now available including combination. Everything compatible with SM.
- Several improvements on the analysis side: particle flow jets, improved categorizations, improved discriminants, improved control regions, more cross sections, more interpretations
- Uncertainty from single channel on inclusive fiducial cross section $\simeq 9\%$
- Uncertainty from single channel on ggF: 10%
VBF: 20-30%, $ttH(\gamma\gamma)$: 35%
- Several STXS 1.2 bins for ggF and VBF at $< 50\%$ from single channel
- Several interpretations on top of the measurement: EFT interpretations based on STXS or differential cross sections
- $H \rightarrow Z\gamma$: 95% CL $3.5\times$ SM. Significance 2.2σ (expected 1.2σ). *Phys. Lett. B* 809 (2020) 135754

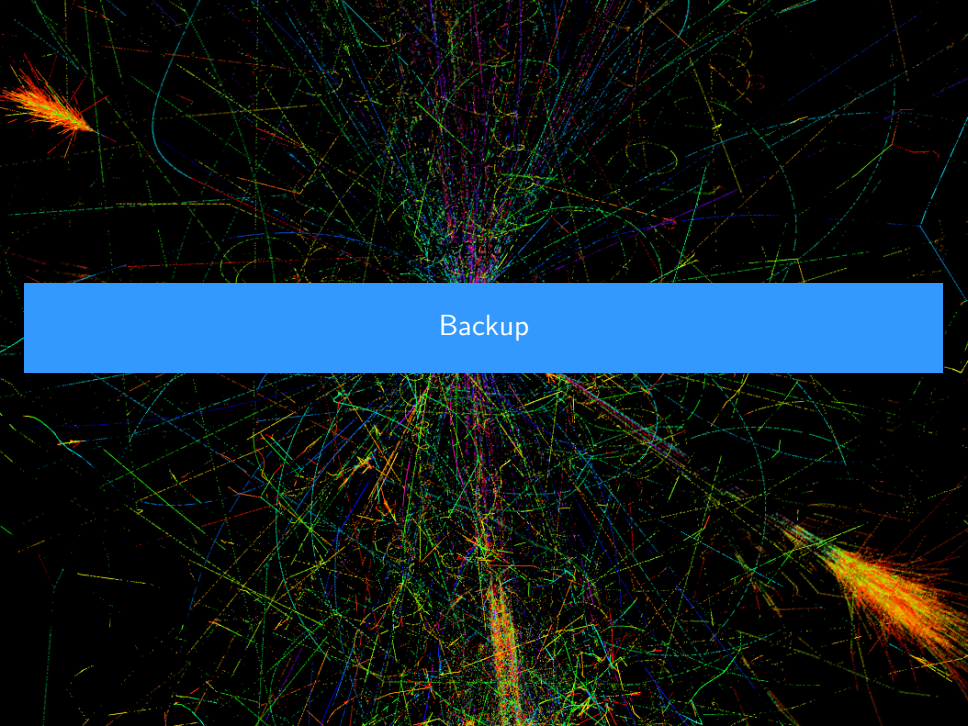


Thanks for your attention





Any questions?

The image features a dense, multi-colored network graph on a black background. The graph consists of numerous nodes and edges, with colors ranging from blue and green to yellow and orange. The edges are thin and form a complex web of connections. There are two prominent, bright orange-yellow clusters of nodes, one in the upper left and one in the lower right, which appear to be hubs or highly connected regions. A solid blue horizontal bar is positioned across the center of the image, containing the word "Backup" in white, sans-serif font.

Backup

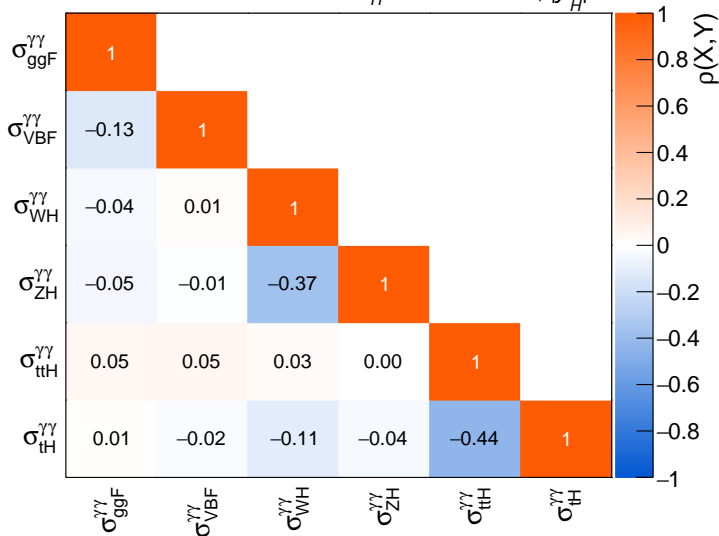
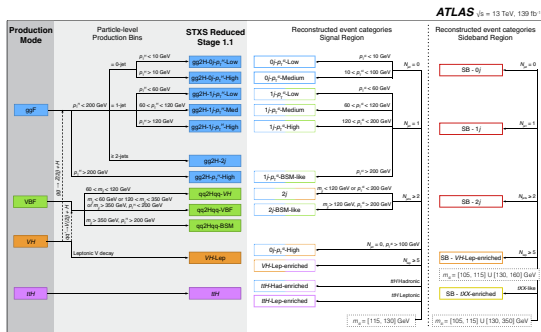
ATLAS
 $\sqrt{s} = 13 \text{ TeV}, 139 \text{ fb}^{-1}$
 $m_H = 125.09 \text{ GeV}, |y_H| < 2.5$


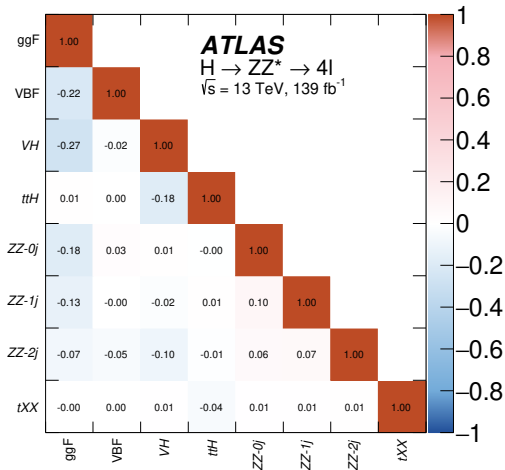
Table 1: Event generators and PDF sets used to model signal and background processes. The cross-sections of Higgs boson production processes are reported for a centre-of-mass energy of $\sqrt{s} = 13$ TeV and a Higgs boson mass of $m_H = 125.09$ GeV. The order of the calculated cross-section is reported in each case. The cross-sections for the background processes are omitted, since the background normalization is determined in fits to the data.

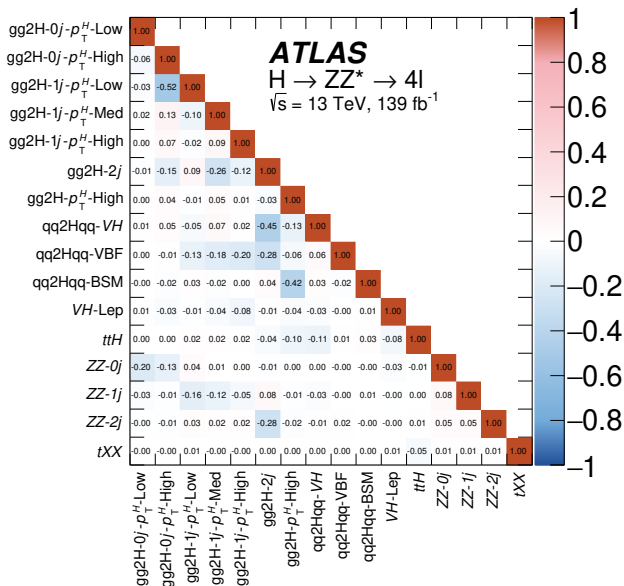
Process	Generator	Showering	PDF set	σ [pb] $\sqrt{s} = 13$ TeV	Order of σ calculation
ggF	NNLOPS	PYTHIA 8.2	PDF4LHC15	48.5	N ³ LO(QCD)+NLO(EW)
VBF	POWHEG BOX	PYTHIA 8.2	PDF4LHC15	3.78	approximate-NNLO(QCD)+NLO(EW)
WH	POWHEG BOX	PYTHIA 8.2	PDF4LHC15	1.37	NNLO(QCD)+NLO(EW)
$qq/qg \rightarrow ZH$	POWHEG BOX	PYTHIA 8.2	PDF4LHC15	0.76	NNLO(QCD)+NLO(EW)
$gg \rightarrow ZH$	POWHEG BOX	PYTHIA 8.2	PDF4LHC15	0.12	NLO(QCD)
$t\bar{t}H$	POWHEG BOX	PYTHIA 8.2	PDF4LHC15	0.51	NLO(QCD)+NLO(EW)
$b\bar{b}H$	POWHEG BOX	PYTHIA 8.2	PDF4LHC15	0.49	NNLO(QCD)
$tHqb$	MADGRAPH5_AMC@NLO	PYTHIA 8.2	NNPDF3.0NNLO	0.074	NLO(QCD)
tHW	MADGRAPH5_AMC@NLO	PYTHIA 8.2	NNPDF3.0NNLO	0.015	NLO(QCD)
$\gamma\gamma$	SHERPA	SHERPA	NNPDF3.0NNLO		
$V\gamma\gamma$	SHERPA	SHERPA	NNPDF3.0NNLO		
$t\bar{t}\gamma\gamma$	MADGRAPH5_AMC@NLO	PYTHIA 8	NNPDF2.3LO		

$\eta_{\gamma_1}, \eta_{\gamma_2}, p_T^{\gamma\gamma}, y_{\gamma\gamma},$
 $p_T^\dagger, m_{jj},$ and $\Delta y, \Delta\phi, \Delta\eta$ between j_1 and $j_2,$
 $p_{T,\gamma\gamma j_1}, m_{\gamma\gamma j_1}, p_{T,\gamma\gamma j_1}^\dagger, m_{\gamma\gamma j_1}$
 $\Delta y, \Delta\phi$ between the $\gamma\gamma$ and jj systems,
 minimum ΔR between jets and photons,
 invariant mass of the system comprising all jets in the event,
 dilepton $p_T,$ di- e or di- μ invariant mass (leptons are required to be oppositely charged),
 E_T^{miss}, p_T and transverse mass of the lepton + E_T^{miss} system,
 p_T, η, ϕ of top-quark candidates, $m_{t_1 t_2}$
 Number of jets †, of central jets ($|\eta| < 2.5$) †, of b -jets † and of leptons,
 p_T of the highest- p_T jet, scalar sum of the p_T of all jets,
 scalar sum of the transverse energies of all particles ($\sum E_T$), E_T^{miss} significance,
 $\left| E_T^{\text{miss}} - E_T^{\text{miss}}(\text{primary vertex with the highest } \sum p_{T,\text{track}}^2) \right| > 30 \text{ GeV}$
 Top reconstruction BDT of the top-quark candidates,
 $\Delta R(W, b)$ of $t_2,$
 $\eta_{j_F}, m_{\gamma\gamma j_F}$
 Average number of interactions per bunch crossing.

STXS classes	Variables
Individual STXS classes from $gg \rightarrow H$ $qq' \rightarrow Hqq'$ $qq \rightarrow H\ell\nu$ $pp \rightarrow H\ell\ell$ $pp \rightarrow H\nu\bar{\nu}$	All multiclass BDT variables, $p_T^{\gamma\gamma}$ projected to the thrust axis of the $\gamma\gamma$ system ($p_{T1}^{\gamma\gamma}$), $\Delta\eta_{\gamma\gamma}, \eta^{\text{ZepP}} = \frac{\eta_{\gamma\gamma} - \eta_{jj}}{2}$, $\phi_{\gamma\gamma}^* = \tan\left(\frac{\pi - \Delta\phi_{\gamma\gamma} }{2}\right) \sqrt{1 - \tanh^2\left(\frac{\Delta\eta_{\gamma\gamma}}{2}\right)}$, $\cos\theta_{\gamma\gamma}^* = \left \frac{(E^{\gamma_1 + p_z^{\gamma_1}) \cdot (E^{\gamma_2 - p_z^{\gamma_2})} - (E^{\gamma_1 - p_z^{\gamma_1}) \cdot (E^{\gamma_2 + p_z^{\gamma_2})})}{m_{\gamma\gamma} + \sqrt{m_{\gamma\gamma}^2 + (p_T^{\gamma\gamma})^2}} \right $ Number of electrons and muons.
all $t\bar{t}H$ and tHW STXS classes combined	p_T, η, ϕ of γ_1 and γ_2 , p_T, η, ϕ and b -tagging scores of the six highest- p_T jets, $E_T^{\text{miss}}, E_T^{\text{miss}}$ significance, E_T^{miss} azimuthal angle, Top reconstruction BDT scores of the top-quark candidates, p_T, η, ϕ of the two highest- p_T leptons.
$tHqb$	$p_T^{\gamma\gamma}/m_{\gamma\gamma}, \eta_{\gamma\gamma}$, p_T , invariant mass, BDT score and $\Delta R(W, b)$ of t_1 , p_T, η of t_2 , p_T, η of j_F , Angular variables: $\Delta\eta_{\gamma\gamma t_1}, \Delta\theta_{\gamma\gamma t_2}, \Delta\theta_{t_1 j_F}, \Delta\theta_{t_2 j_F}, \Delta\theta_{\gamma\gamma j_F}$ Invariant mass variables: $m_{\gamma\gamma j_F}, m_{t_1 j_F}, m_{t_2 j_F}, m_{\gamma\gamma t_1}$ Number of jets with $p_T > 25$ GeV, Number of b -jets with $p_T > 25$ GeV*; Number of leptons*, E_T^{miss} significance*



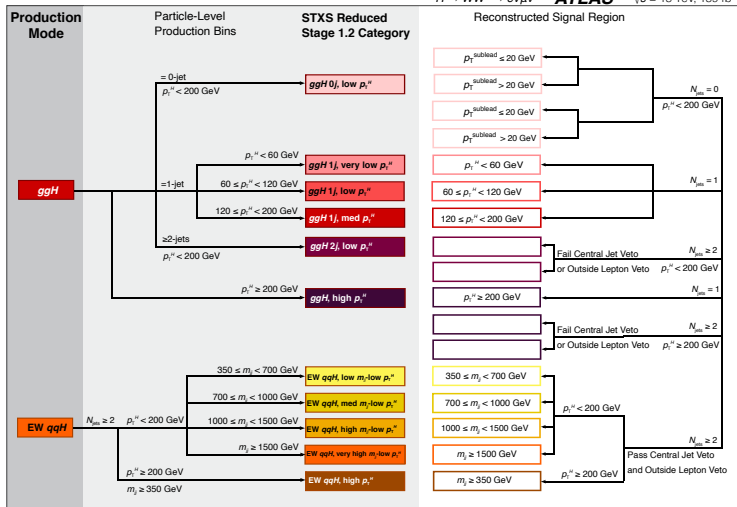




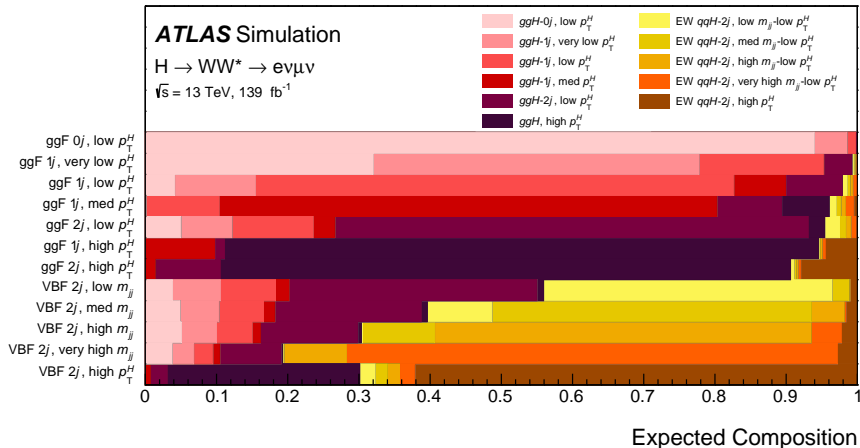
TRIGGER	
Combination of single-lepton, dilepton and trilepton triggers	
LEPTONS AND JETS	
ELECTRONS	$E_T > 7 \text{ GeV}$ and $ \eta < 2.47$
MUONS	$p_T > 5 \text{ GeV}$ and $ \eta < 2.7$, calorimeter-tagged: $p_T > 15 \text{ GeV}$
JETS	$p_T > 30 \text{ GeV}$ and $ \eta < 4.5$
QUADRUPLETS	
All combinations of two same-flavour and opposite-charge lepton pairs	
- Leading lepton pair: lepton pair with invariant mass m_{l_2} closest to the Z boson mass m_Z	
- Subleading lepton pair: lepton pair with invariant mass m_{l_4} second closest to the Z boson mass m_Z	
Classification according to the decay final state: $4\mu, 2e2\mu, 2\mu2e, 4e$	
REQUIREMENTS ON EACH QUADRUPLET	
LEPTON	- Three highest- p_T leptons must have p_T greater than 20, 15 and 10 GeV
RECONSTRUCTION	- At most one calorimeter-tagged or stand-alone muon
LEPTON PAIRS	- Leading lepton pair: $50 < m_{l_2} < 106 \text{ GeV}$ - Subleading lepton pair: $m_{\text{min}} < m_{l_4} < 115 \text{ GeV}$ - Alternative same-flavour opposite-charge lepton pair: $m_{\ell\ell} > 5 \text{ GeV}$ - $\Delta R(\ell, \ell') > 0.10$ for all lepton pairs
LEPTON ISOLATION	- The amount of isolation E_T after summing the track-based and 40% of the calorimeter-based contribution must be smaller than 16% of the lepton p_T
IMPACT PARAMETER	- Electrons: $ d_0 /\sigma(d_0) < 5$
SIGNIFICANCE	- Muons: $ d_0 /\sigma(d_0) < 3$
COMMON VERTEX	- χ^2 -requirement on the fit of the four lepton tracks to their common vertex
SELECTION OF THE BEST QUADRUPLET	
- Select quadruplet with m_{l_2} closest to m_Z from one decay final state in decreasing order of priority: $4\mu, 2e2\mu, 2\mu2e$ and $4e$	
- If at least one additional (fifth) lepton with $p_T > 12 \text{ GeV}$ meets the isolation, impact parameter and angular separation criteria, select the quadruplet with the highest matrix-element value	
HIGGS BOSON MASS WINDOW	
- Correction of the four-lepton invariant mass due to the FSR photons in Z boson decays	
- Four-lepton invariant mass window in the signal region: $115 < m_{4\ell} < 130 \text{ GeV}$	
- Four-lepton invariant mass window in the sideband region: $105 < m_{4\ell} < 115 \text{ GeV}$ or $130 < m_{4\ell} < 160 (350) \text{ GeV}$	

Category	Processes	MLP	Lepton RNN	Jet RNN	Discriminant
0j- $p_T^{\ell\ell}$ -Low	ggF, ZZ*	$p_T^{\ell\ell}, D_{ZZ}, m_{12}, m_{34},$	p_T^{ℓ}, η_{ℓ}	-	NN _{ggF}
0j- $p_T^{\ell\ell}$ -Med		$ \cos \theta^* , \cos \theta_1, \phi_{ZZ}$			
1j- $p_T^{\ell\ell}$ -Low	ggF, VBF, ZZ*	$p_T^{\ell\ell}, p_T^j, \eta_j,$ $\Delta R_{4\ell j}, D_{ZZ},$	p_T^{ℓ}, η_{ℓ}	-	NN _{VBF} for NN _{ZZ} < 0.25
1j- $p_T^{\ell\ell}$ -Med		$p_T^{\ell\ell}, p_T^j, \eta_j, E_T^{\text{miss}},$ $\Delta R_{4\ell j}, D_{ZZ}, \eta_{4\ell}$			NN _{ZZ} for NN _{ZZ} > 0.25
1j- $p_T^{\ell\ell}$ -High	ggF, VBF	$p_T^{\ell\ell}, p_T^j, \eta_j,$ $E_T^{\text{miss}}, \Delta R_{4\ell j}, \eta_{4\ell}$	p_T^{ℓ}, η_{ℓ}	-	NN _{VBF}
2j	ggF, VBF, VH	$m_{jj}, p_T^{\Delta\ell jj}$	p_T^{ℓ}, η_{ℓ}	p_T^j, η_j	NN _{VBF} for NN _{VH} < 0.2
2j-BSM-like		$\eta_{ZZ}^{\text{Zpp}}, p_T^{\Delta\ell jj}$			NN _{VH} for NN _{VH} > 0.2
VH-Lep-enriched	VH, ttH	$N_{\text{jets}}, N_{b\text{-jets},70\%},$ E_T^{miss}, H_T	p_T^{ℓ}	-	NN _{ttH}
ttH-Had-enriched	ggF, ttH, tXX	$p_T^{\ell\ell}, m_{jj},$ $\Delta R_{4\ell j}, N_{b\text{-jets},70\%},$	p_T^{ℓ}, η_{ℓ}	p_T^j, η_j	NN _{ttH} for NN _{tXX} < 0.4 NN _{tXX} for NN _{tXX} > 0.4

$H \rightarrow WW^* \rightarrow e\nu\mu\nu$ **ATLAS** $\sqrt{s} = 13$ TeV, 139 fb⁻¹



Reconstructed Signal Region



Process	Matrix element (alternative)	PDF set	UEPS model (alternative model)	Prediction order for total cross section
ggF H	POWHEG BOX v2 NNLOPS (MG5_AMC@NLO)	PDF4LHC15NNLO	PYTHIA 8 (HERWIG 7)	N ³ LO QCD + NLO EW
VBF H	POWHEG BOX v2 (MG5_AMC@NLO)	PDF4LHC15NLO	PYTHIA 8 (HERWIG 7)	NNLO QCD + NLO EW
VH excl. $gg \rightarrow ZH$	POWHEG BOX v2	PDF4LHC15NLO	PYTHIA 8	NNLO QCD + NLO EW
$t\bar{t}H$	POWHEG BOX v2	NNPDF3.0NLO	PYTHIA 8	NLO
$gg \rightarrow ZH$	POWHEG BOX v2	PDF4LHC15NLO	PYTHIA 8	NNLO QCD + NLO EW
$qq \rightarrow WW$	SHERPA 2.2.2	NNPDF3.0NNLO	SHERPA 2.2.2 (SHERPA 2.2.2 ; μ_q)	NLO
$qq \rightarrow WWqq$	MG5_AMC@NLO	NNPDF3.0NLO	PYTHIA 8 (HERWIG 7)	LO
$gg \rightarrow WW/ZZ$	SHERPA 2.2.2	NNPDF3.0NNLO	SHERPA 2.2.2	NLO
$WZ/V\gamma^*/ZZ$	SHERPA 2.2.2	NNPDF3.0NNLO	SHERPA 2.2.2	NLO
$V\gamma$	SHERPA 2.2.8	NNPDF3.0NNLO	SHERPA 2.2.8	NLO
VVV	SHERPA 2.2.2	NNPDF3.0NNLO	SHERPA 2.2.2	NLO
$t\bar{t}$	POWHEG BOX v2 (MG5_AMC@NLO)	NNPDF3.0NLO	PYTHIA 8 (HERWIG 7)	NNLO+NNLL
Wt	POWHEG BOX v2 (MG5_AMC@NLO)	NNPDF3.0NLO	PYTHIA 8 (HERWIG 7)	NNLO
Z/γ^*	SHERPA 2.2.1 (MG5_AMC@NLO)	NNPDF3.0NNLO	SHERPA 2.2.1	NNLO

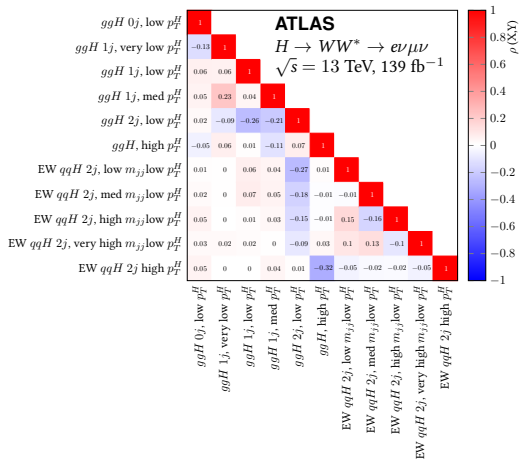
Source	$\frac{\Delta\sigma_{ggF+VBF}\cdot\mathcal{B}_{H\rightarrow WW^*}}{\sigma_{ggF+VBF}\cdot\mathcal{B}_{H\rightarrow WW^*}}$ [%]	$\frac{\Delta\sigma_{ggF}\cdot\mathcal{B}_{H\rightarrow WW^*}}{\sigma_{ggF}\cdot\mathcal{B}_{H\rightarrow WW^*}}$ [%]	$\frac{\Delta\sigma_{VBF}\cdot\mathcal{B}_{H\rightarrow WW^*}}{\sigma_{VBF}\cdot\mathcal{B}_{H\rightarrow WW^*}}$ [%]
Data statistical uncertainties	4.6	5.1	15
Total systematic uncertainties	9.5	11	18
MC statistical uncertainties	3.0	3.8	4.9
Experimental uncertainties	5.2	6.3	6.7
Flavor tagging	2.3	2.7	1.0
Jet energy scale	0.9	1.1	3.7
Jet energy resolution	2.0	2.4	2.1
E_T^{miss}	0.7	2.2	4.9
Muons	1.8	2.1	0.8
Electrons	1.3	1.6	0.4
Fake factors	2.1	2.4	0.8
Pileup	2.4	2.5	1.3
Luminosity	2.1	2.0	2.2
Theoretical uncertainties	6.8	7.8	16
ggF	3.8	4.3	4.6
VBF	3.2	0.7	12
WW	3.5	4.2	5.5
Top	2.9	3.8	6.4
$Z\tau\tau$	1.8	2.3	1.0
Other VV	2.3	2.9	1.5
Other Higgs	0.9	0.4	0.4
Background normalizations	3.6	4.5	4.9
WW	2.2	2.8	0.6
Top	1.9	2.3	3.4
$Z\tau\tau$	2.7	3.1	3.4
Total	10	12	23

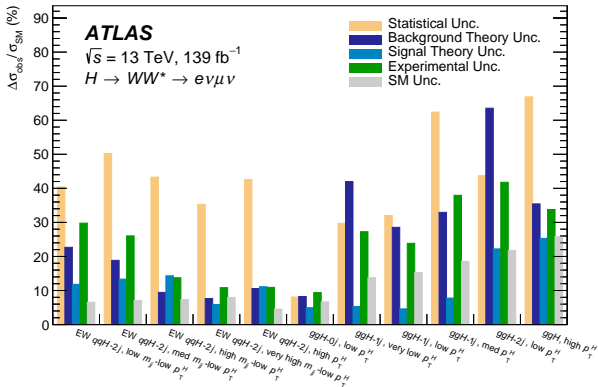
WW signal regions selection

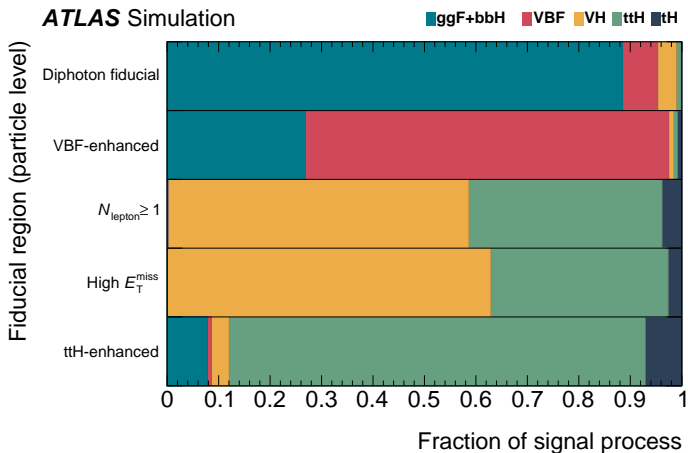
Category	$N_{\text{jet},(p_T > 30 \text{ GeV})} = 0$ ggF	$N_{\text{jet},(p_T > 30 \text{ GeV})} = 1$ ggF	$N_{\text{jet},(p_T > 30 \text{ GeV})} \geq 2$ ggF	$N_{\text{jet},(p_T > 30 \text{ GeV})} \geq 2$ VBF
Preselection	Two isolated, different-flavor leptons ($\ell = e, \mu$) with opposite charge			
	$p_T^{\text{lead}} > 22 \text{ GeV}$, $p_T^{\text{sublead}} > 15 \text{ GeV}$ $m_{\ell\ell} > 10 \text{ GeV}$			
	$p_T^{\text{miss}} > 20 \text{ GeV}$			
Background rejection	$N_{b\text{-jet},(p_T > 20 \text{ GeV})} = 0$			
	$\Delta\phi_{\ell\ell, E_T^{\text{miss}}} > \pi/2$	$m_{\tau\tau} < m_Z - 25 \text{ GeV}$		
	$p_T^{\ell\ell} > 30 \text{ GeV}$	$\max(p_T^{\ell}) > 50 \text{ GeV}$		
$H \rightarrow WW^* \rightarrow e\nu\mu\nu$ topology	$m_{\ell\ell} < 55 \text{ GeV}$			central jet veto outside lepton veto $m_{jj} > 120 \text{ GeV}$
	$\Delta\phi_{\ell\ell} < 1.8$			
		fail central jet veto or fail outside lepton veto		
		$ m_{jj} - 85 > 15 \text{ GeV}$ or $\Delta y_{jj} > 1.2$		
Discriminating fit variable	m_T			DNN

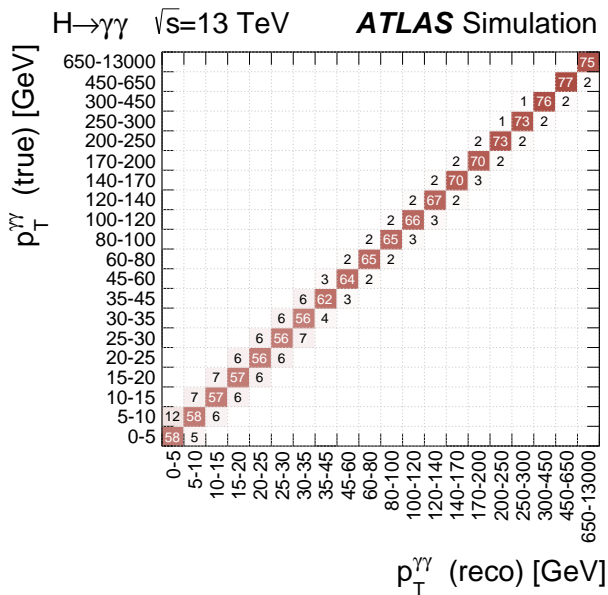
WW control regions selection

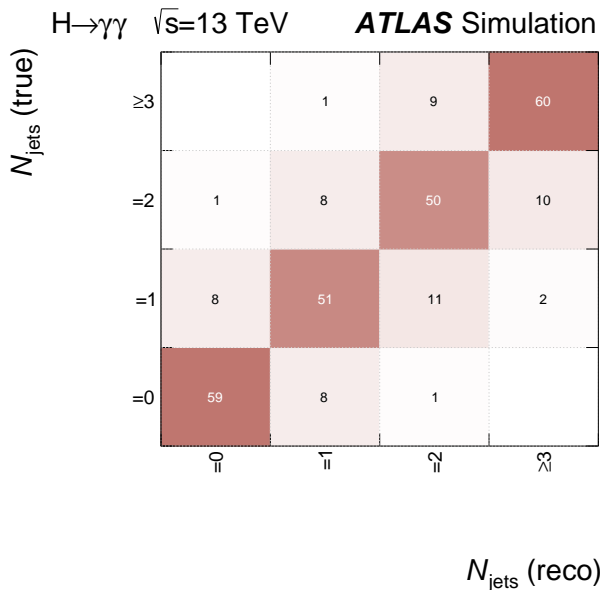
CR	$N_{\text{jet},(p_T>30 \text{ GeV})} = 0$ ggF	$N_{\text{jet},(p_T>30 \text{ GeV})} = 1$ ggF	$N_{\text{jet},(p_T>30 \text{ GeV})} \geq 2$ ggF	$N_{\text{jet},(p_T>30 \text{ GeV})} \geq 2$ VBF
$qq \rightarrow WW$	$N_{b\text{-jet},(p_T>20 \text{ GeV})} = 0$			
	$\Delta\phi_{\ell\ell, E_{\text{T}}^{\text{miss}}} > \pi/2$ $p_T^{\ell\ell} > 30 \text{ GeV}$ $55 < m_{\ell\ell} < 110 \text{ GeV}$ $\Delta\phi_{\ell\ell} < 2.6$	$m_{\ell\ell} > 80 \text{ GeV}$		
		$ m_{\tau\tau} - m_Z > 25 \text{ GeV}$ $\max(m_{\tau\tau}^{\ell}) > 50 \text{ GeV}$	$m_{\tau\tau} < m_Z - 25 \text{ GeV}$ $m_{\tau 2} > 165 \text{ GeV}$	
			fail central jet veto or fail outside lepton veto $ m_{jj} - 85 > 15 \text{ GeV}$ or $\Delta y_{jj} > 1.2$	
<hr/>				
$t\bar{t}/Wt$	$N_{b\text{-jet},(20 < p_T < 30 \text{ GeV})} > 0$ $\Delta\phi_{\ell\ell, E_{\text{T}}^{\text{miss}}} > \pi/2$ $p_T^{\ell\ell} > 30 \text{ GeV}$ $\Delta\phi_{\ell\ell} < 2.8$	$N_{b\text{-jet},(p_T>30 \text{ GeV})} = 1$ $N_{b\text{-jet},(20 < p_T < 30 \text{ GeV})} = 0$	$N_{b\text{-jet},(p_T>20 \text{ GeV})} = 0$	$N_{b\text{-jet},(p_T>20 \text{ GeV})} = 1$
		$m_{\tau\tau} < m_Z - 25 \text{ GeV}$		central jet veto outside lepton veto
		$\max(m_{\tau\tau}^{\ell}) > 50 \text{ GeV}$	$m_{\ell\ell} > 80 \text{ GeV}$ $\Delta\phi_{\ell\ell} < 1.8$ $m_{\tau 2} < 165 \text{ GeV}$	
			fail central jet veto or fail outside lepton veto $ m_{jj} - 85 > 15 \text{ GeV}$ or $\Delta y_{jj} > 1.2$	
<hr/>				
Z/γ^*	$N_{b\text{-jet},(p_T>20 \text{ GeV})} = 0$			
	$m_{\ell\ell} < 80 \text{ GeV}$ no p_T^{miss} requirement		$m_{\ell\ell} < 55 \text{ GeV}$	$m_{\ell\ell} < 70 \text{ GeV}$
	$\Delta\phi_{\ell\ell} > 2.8$	$m_{\tau\tau} > m_Z - 25 \text{ GeV}$		$ m_{\tau\tau} - m_Z \leq 25 \text{ GeV}$ central jet veto outside lepton veto
		$\max(m_{\tau\tau}^{\ell}) > 50 \text{ GeV}$	fail central jet veto or fail outside lepton veto $ m_{jj} - 85 > 15 \text{ GeV}$ or $\Delta y_{jj} > 1.2$	
<hr/>				

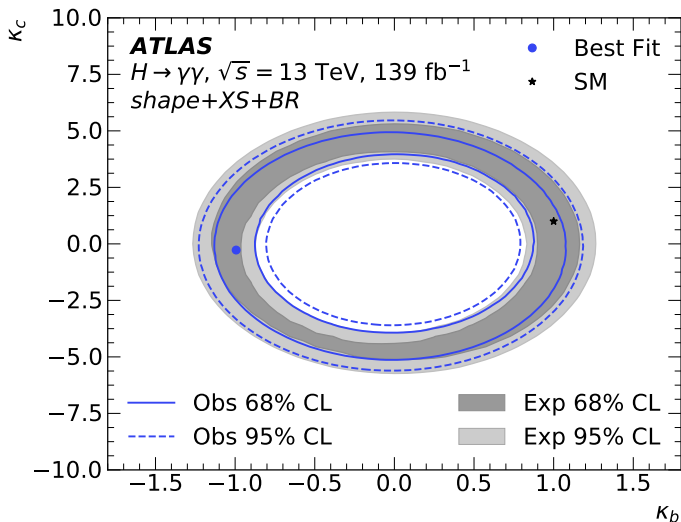












Source	Uncertainty [%]
Statistical uncertainty	7.5
Systematic uncertainties	6.4
Background modelling (spurious signal)	3.8
Photon energy scale & resolution	3.6
Photon selection efficiency	2.6
Luminosity	1.8
Pile-up modelling	1.4
Trigger efficiency	1.0
Theoretical modelling	0.4
Total	9.8

Standard Model Production Cross Section Measurements

Status: February 2022

